Macromolecules

Article

pubs.acs.org/Macromolecules

Thieno[3,4-*b*]thiophene Acceptors with Alkyl, Aryl, Perfluoroalkyl, and Perfluorophenyl Pendants for Donor−Acceptor Low Bandgap Polymers

Patrick D. Homyak,[†] Jonathan Tinkham,[‡] Paul M. Lahti,[‡] and E. Bryan Coughlin*[,†]

[†]Department of Polymer Science & Engineering, University of Massachusetts, Conte Center for Polymer Research, 120 Governors Drive, Amherst, Massachusetts 01003, United States

[‡]Department of Chemistry, University of Massachusetts—Amherst, 710 North Pleasant St., Amherst, Massachusetts 01003, United States

Supporting Information

ABSTRACT: We report the design, synthesis, and characterization of a series of thieno[3,4-*b*]thiophene acceptor blocks with octyl (T8), phenyl (TP), perfluorooctyl (TF8), and perfluorophenyl (TFP) side groups. Their subsequent copolymerization with dithienylbenzodithiophene by direct arylation polymerization afforded novel low bandgap poly(thienothiophene-*alt*-dithienylbenzodithiophene) (PTB) polymers. The strongly electron withdrawing TF8 and TFP groups were shown to significantly lower both E_{HOMO} and E_{LUMO} levels and gave computed copolymer ground-to-excited state dipole changes ($\Delta\mu_{ge}$) that were relatively higher than for the nonfluorinated analogues. These materials show favorably aligned energy levels relative to conventional fullerene-type acceptors, which should allow them to perform well in organic photovoltaics.

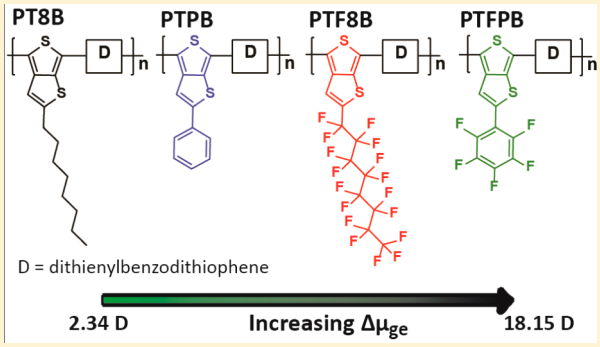

1. INTRODUCTION

Design, preparation, and characterization of new conjugated polymers has received increased attention over the past two decades due to their potential to serve as semiconducting materials for relatively low-cost, thin, flexible organic electronics such as organic photovoltaics (OPVs), organic field-effect transistors (OFETs), and organic light-emitting diodes (OLEDs).[1,2] This concentrated research effort has led to significant improvements in the understanding and design of conjugated systems, which in the case of OPVs has resulted in vastly improved device efficiencies. Specifically, single junction OPVs have been reported to have power conversion efficiencies (PCEs) consistently around 6−8% and tandem junction devices with PCEs approaching and now exceeding 10%.[3−10]

The design of polymers with appropriate electrochemical and structural properties to improve OPV efficiencies has been a central research focus of numerous research groups. Low bandgap polymers have been engineered to have appropriately aligned E_{HOMO}/E_{LUMO} electronic levels relative to PCBM, optimized side chains to enhance solubility while enabling good interchain interactions, good crystallinity/planarity through the backbone to promote high charge mobility, and low bandgaps (E_g) to increase the harvested range of the solar spectrum.

Recent developments have focused on incorporating fluorine atoms onto the acceptor unit in the backbone of donor−acceptor (D−A) alternating copolymers. It has been demonstrated that the incorporation of a single fluorine atom can have drastic effects not only on the electrochemical properties of the polymer but also on chain packing and orientation as well as interpolymer interactions and miscibility with PCBM.[3] These effects have been shown to give significant absolute increases in the PCE ranging from 1% to 2%. Several reports of polymers with mono- or difluorinated acceptor units have yielded similar observations.[11] While it has been shown that fluorinated polymers are quite advantageous for various uses due to superior performance and enhanced stability, it is not entirely clear what fundamental changes arise from fluorine substitution to create these favorable properties.

Several observations have been made regarding both the electrical and morphological changes induced upon incorporation of fluorine on the acceptor unit in a D−A conjugated polymer backbone. First, both E_{HOMO} and E_{LUMO} are lowered, leading to enhanced open-circuit voltage (V_{oc}) due to the increased $E^{polymer}_{HOMO}/E^{PCBM}_{LUMO}$ energy offset. Second, the ground-to-excited state dipole change ($\Delta\mu_{ge}$) is increased,[12] decreasing geminate recombination by allowing more efficient charge separation and increasing both the external quantum efficiency (EQE) and internal quantum efficiency (IQE) for harvesting

Received: September 19, 2013
Revised: October 17, 2013
Published: November 4, 2013

   dx.doi.org/10.1021/ma4019476 | *Macromolecules* 2013, 46, 8873−8881

charges. Studies have suggested a strong correlation between computational values for $\Delta\mu_{ge}$ and observed PCE.[12a,b]

Upon fluorine substitution on a conjugated chain, the morphology of the system can be drastically altered. Strong Ar−F···Ar and C−H···F interactions can occur in the solid state,[13] leading to enhanced packing (smaller interchain distance) and a more face-on orientation,[14] which enhances solar cell charge mobility, short-circuit current (J_{sc}), and fill factor (FF). Fluorophobicity of PCBM decreases the miscibility of PCBM in the bulk polymer,[15] leading to enhanced purity of both PCBM and bulk polymer domains, which ultimately increases charge transport and decreases bimolecular recombination. Of these multiple factors, it is not immediately clear which effect is the most important and should be exploited to create higher performing devices for a given device configuration.

Studies of conjugated polymers with fluorine substitution are necessary to elucidate how these effects balance one another and to investigate how these systems may be further improved to increase PCEs. We report the design, synthesis, and preliminary characterization of a new series of alternating thieno[3,4-*b*]thiophene dithienyl-substituted benzodithiophene polymers which utilize the D−A alternating copolymer approach for achieving low bandgap materials. In order to study the effects of fluorination, thienothiophene monomers were synthesized with octyl (T8), phenyl (TP), perfluorooctyl (TF8), and perfluorophenyl (TFP) substituents, as shown in Figure 1. Polymerization of these monomers with benzodithiophene by direct arylation polymerization yielded the corresponding PT8B, PTPB, PTF8B, and PTFPB alternating D−A copolymers (Figure 2). Direct arylation polymerization utilizes activated aromatic C−H bonds and aryl halides to produce new Ar−Ar bonds.[16] This method has been shown to produce a variety of reasonable molecular weight polymers with good alternating linear structure, while eliminating the need for extra synthetic steps which are normally required for other strategies such as Stille or Suzuki polycondensation.[17] To our knowledge, this is the first example of thieno[3,4-*b*]thiophene polymerization by direct arylation.

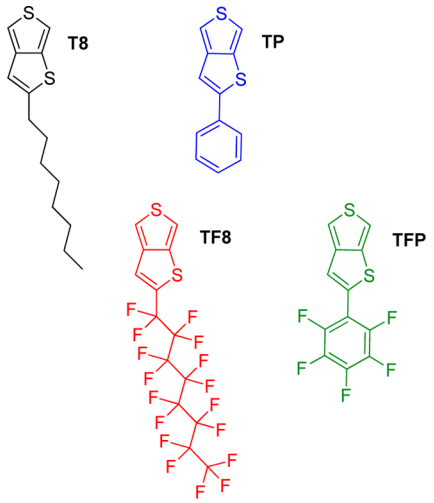

Figure 1. Thieno[3,4-*b*]thiophene monomeric units: T8, TP, TF8, and TFP.

2. EXPERIMENTAL SECTION

2.1. Materials. All reagents and chemicals were purchased from commercial sources (Matrix Scientific, Sigma-Aldrich, Acros Organics, Alfa Aesar) and used without further purification unless stated otherwise. 4,6-Dihydrothieno[3,4-*b*]thiophene (3),[18] potassium pentafluorobenzoate,[19] and 4,8-bis(5-(2-ethylhexyl)thiophen-2-yl)benzo[1,2-*b*;4,5-*b*′]dithiophene (7)[20] were all synthesized using previously reported methods. All reactions were performed under an inert (N_2) atmosphere. Tetrahydrofuran (THF) was distilled over sodium prior to use.

2.2. Characterization. ^{1}H and ^{19}F NMR spectra were collected with a 300 MHz Bruker Spectrospin or a 400 MHz Agilent Technologies Varian instrument with variable temperature capability. ^{13}C NMR spectra were collected on a 100 MHz Bruker Spectrospin instrument. UV−vis absorption measurements of polymer solutions and films were performed on a PerkinElmer Lamba 25 UV−vis spectrometer. Films for absorption spectra were spin-coated from 10 mg/mL polymer solutions in $CHCl_3$ at 1500 rpm for 60 s. Film thicknesses was determined using a KLA Tencor Alpha Step IQ surface profiler. Polymer molecular weight and dispersity ($Đ$) analysis was completed via gel-permeation chromatography (GPC) in 1,2,4-trichlorobenzene at 135 °C using a Polymer Laboratories PL-220 high-temperature GPC instrument calibrated against polystyrene standards. MALDI-TOF experiments were performed on a Bruker microflex instrument, using terthiophene as the ionizing matrix (1:1000 to 1:5000 w/w polymer to matrix). Cyclic voltammetry (CV) measurements of the polymer films were done with a Bioanalytical Systems Inc. (BASi) EC Epsilon potentiostat using a three-electrode configuration consisting of a glassy carbon working electrode, a Ag/$AgNO_3$ (0.01 M in acetonitrile) reference electrode, and a Pt wire counter electrode in tetrabutylammonium hexafluorophosphate electrolyte solution (0.1 M) in acetonitrile. Measurements were calibrated to the ferrocene/ferrocenium redox couple (Fc/Fc^+) as an external reference. Films for CV were drop-cast directly onto the glassy carbon working electrode from 2.5 mg/mL polymer solutions in $CHCl_3$.

2.3. Synthesis. *Compound 1.* Into a clean, dry 250 mL two-neck flask with condenser was added $Pd(PPh_3)Cl_2$ (2.176 g, 3.10 mmol) and CuI (0.590 g, 3.10 mmol) followed by N_2 purging. Then 3,4-dibromothiophene (15 g, 62.00 mmol), decyne (8.697 g, 62.00 mmol), diisopropylamine (60 mL), and methanol (60 mL) were added sequentially. The reaction was heated to 85 °C for 48 h. After cooling to room temperature, the reaction mixture was diluted with ether, washed with H_2O and brine, dried with $MgSO_4$, and concentrated. Purification by column chromatography (hexanes) yielded **1** (8.090 g, 44%) as viscous yellow liquid. ^{1}H NMR (300 MHz, $CDCl_3$): 7.35 (1 H, d, J = 3 Hz), 7.22 (1 H, d, J = 3 Hz), 2.46 (2 H, t, 7 Hz), 1.67 (2 H, m), 1.52 (2 H, m), 1.33 (8 H, m), 0.930 (3 H, t, J = 6 Hz). ^{13}C NMR (100 MHz, $CDCl_3$): 127.75, 125.28, 122.56, 113.96, 93.65, 74.09, 31.95, 29.32, 29.21, 28.94, 28.68, 22.77, 19.51, 14.22. GC-MS (m/z): Found 300 (Calcd 298.04, 300.04 for [$C_{14}H_{19}BrS$]).

Compound 2. Into a clean, dry 250 mL two-neck flask with condenser was added $Pd(PPh_3)Cl_2$ (2.176 g, 3.10 mmol) and CuI (0.590 g, 3.10 mmol) followed by N_2 purging. Then 3,4-dibromothiophene (15 g, 62.00 mmol), phenylacetylene (6.759 g, 62.00 mmol), diisopropylamine (60 mL), and methanol (60 mL) were added sequentially. The reaction was heated to 85 °C for 48 h. After cooling to room temperature, the reaction mixture was diluted with ether, washed with H_2O and brine, dried with $MgSO_4$, and concentrated. Purification by column chromatography (hexanes) yielded a white solid **2** (6.940 g, 43%). ^{1}H NMR (400 MHz, CD_2Cl_2): 7.61−7.58 (3 H, m), 7.43−7.38 (4 H, m). ^{13}C NMR (100 MHz, CD_2Cl_2): 149.74, 147.92, 138.10, 134.67, 128.90, 128.54, 126.05, 112.42, 112.25, 110.82. GC-MS (m/z): Found 264 (Calcd 261.95, 263.94 for [$C_{12}H_7BrS$]).

Compound M1. Into a 1 L flask with condenser was added sodium sulfide nonahydrate (12.99 g, 54.07 mmol), copper oxide nanoparticles (0.1075 g, 1.35 mmol), **1** (8.090 g, 27.032 mmol), and NMP (500 mL, 0.05 M). The reaction was heated to 190 °C for 24 h and then cooled

dx.doi.org/10.1021/ma4019476 | *Macromolecules* 2013, 46, 8873−8881

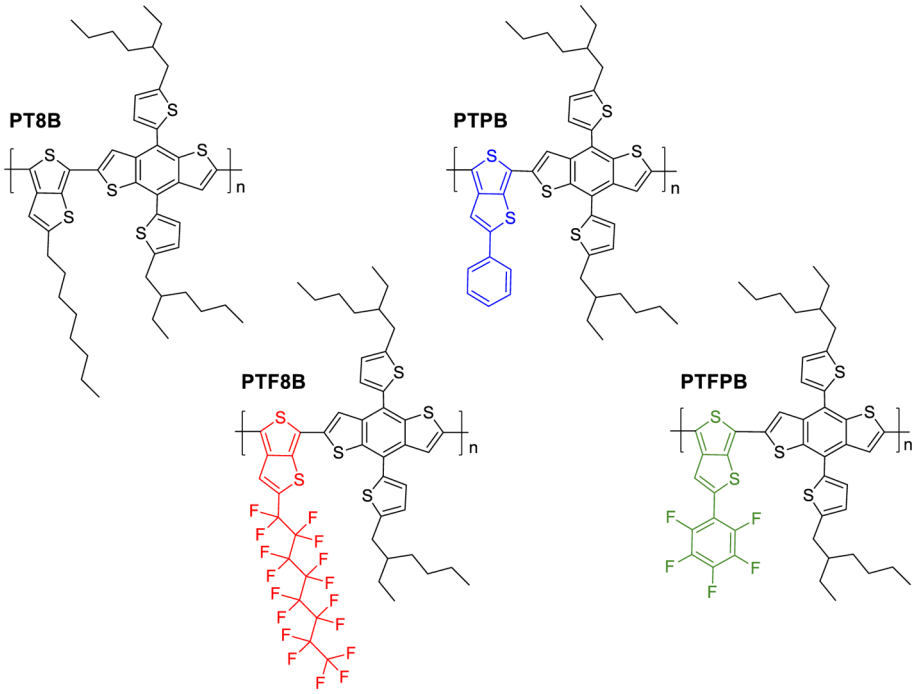

Figure 2. Poly(thieno[3,4-*b*]thiophene-*alt*-dithienylbenzodithiophene) (PTB) series.

to room temperature. The reaction mixture was poured into water, extracted with ethyl acetate, washed with water and brine, dried with $MgSO_4$, and concentrated under reduced pressure. Purification by column chromatography (hexanes) yielded an orange-yellow viscous liquid **M1** (2.98 g, 44%). ^{1}H NMR (300 MHz, $CDCl_3$): 7.19 (2 H, s), 6.66 (1 H, s), 2.79 (2 H, t, J = 7 Hz), 1.70 (2 H, m), 1.35 (10 H, m), 0.92 (3 H, m), 0.93 (3 H, t, J = 6 Hz). ^{13}C NMR (75 MHz, $CDCl_3$): 125.75, 125.28, 122.56, 113.96, 93.65, 74.09, 31.95, 29.32, 29.21, 28.94, 28.68, 22.77, 19.51, 14.22. MS (EI+, m/z): Found 252.101 (Calcd 252.100 for $[C_{14}H_{20}S_2]$.

Compound M2. Into a 1 L flask with condenser was added sodium sulfide nonahydrate (12.99 g, 54.07 mmol), copper oxide nanopowder (0.1075 g, 1.35 mmol, <50 nm), **2** (6.940 g, 52.75 mmol), and *N*-methylpyrrolidinone (NMP, 500 mL, 0.05 M). The reaction was heated to 190 °C for 24 h and then cooled to room temperature. The reaction mixture was poured into water, extracted with ethyl acetate, washed with water and brine, dried with $MgSO_4$, and concentrated under reduced pressure. Purification by column chromatography (hexanes) yielded a white solid which was recrystallized in ethanol to yield a white crystalline solid **M2** (1.25 g, 22%). ^{1}H NMR (300 MHz, $CDCl_3$): 7.66 (2 H, d), 7.54–7.28 (5 H, m). ^{13}C NMR (75 MHz, $CDCl_3$): 149.72, 147.92, 138.16, 134.68, 128.90, 128.54, 126.05, 112.42, 112.23, 110.82. MS (EI+, m/z): Found 216.007; Calcd 216.0067 for $[C_{12}H_8S_2]$.

Compound 4. Into a 250 mL two-neck flask was added **3** (2.00 g, 14.09 mmol) and $CHCl_3$:AcOH (1:1 ratio, 140 mL, 0.1 M) while the reaction flask was shielded from light. The reaction flask was then degassed with N_2 for 15 min followed by addition of solid *N*-bromosuccinimide (2.63 g, 14.79 mmol) and stirring for 3 h. H_2O (100 mL) was then added, and the mixture was extracted with dichloromethane (DCM). The organic layer was separated and washed with H_2O, dried with $MgSO_4$, and concentrated under reduced pressure yielding **4** (quantitative yield) as a dark orange-brown oily solid, which was relatively unstable under ambient conditions and used immediately. ^{1}H NMR (300 MHz, CD_2Cl_2): 6.85 (1 H, s), 4.15 (2 H, s), 4.06 (2 H, s). ^{13}C NMR (75 MHz, CD_2Cl_2): 142.50, 139.20, 124.86, 113.75, 33.90, 33.80. GC-MS (m/z): Found 221 g/mol (Calcd 219.90, 221.90 for $[C_6H_5BrS_2]$).

Compound 5. Into a clean, dry 250 mL two-neck flask with condenser was added copper–tin alloy (1.978 g, 10.85 mmol) and anhydrous dimethyl sulfoxide (DMSO, 28 mL, 0.4 M), which was stirred at 125 °C for 15 min. Perfluorooctyl iodide (2.96 g, 5.43 mmol) was added then in one portion, and the mixture was stirred for 30 min. Compound **4** (1 g, 4.52 mmol) in DMSO (28 mL, 0.15 M) was added dropwise, and the mixture was stirred for 24 h. After completion, the reaction was cooled to room temperature and quenched with H_2O (60 mL). Ether was added, and the mixture was filtered through Celite. The ether layer was separated, and the aqueous layer was extracted with more ether. The combined ether layers were washed with H_2O, dried over anhydrous $MgSO_4$, and concentrated under reduced pressure. The product was purified by column chromatography (hexane/DCM), yielding orange solid **5** (290 mg, 11%). ^{1}H NMR (300 MHz, CD_2Cl_2): 7.19 (1 H, s), 4.25 (2 H, s), 4.11 (2 H, s). ^{19}F NMR (300 MHz, CD_2Cl_2): 81.42 (3 F, t), 102.10 (2 F, t), 121.58–122.25 (8 F, m), 123.09 (2 F, s), 126.54 (2 F, t).

Compound M3. Compound **5** (266 mg, 0.474 mmol) was placed in a 20 mL vial with septa and purged with N_2. DCM (6 mL, 0.08 M) was added, and the reaction mixture was cooled to 0 °C. 2,3-Dichloro-5,6-dicyanobenzoquinone (DDQ, 215 mg, 0.948 mmol) was added as a solid under a stream of N_2. After 1.5 h the solvent was removed, and the product was purified by column chromatography (hexanes/DCM) yielding white solid **M3** (153 mg, 56%). ^{1}H NMR (300 MHz, CD_2Cl_2): 7.68 (1 H, d), 7.44 (1 H, d), 7.41 (1 H, s). ^{19}F NMR (300 MHz, CD_2Cl_2): 81.42 (3 F, t), 104.03 (2 F, m), 121.46–122.90 (8 F, m), 122.90 (2 F, s), 126.32 (2 F, t). MS (FAB+, m/z): 557.941, Calcd 557.9405 for $[C_{14}H_3F_{17}S_2]$.

Compound 6. Into a clean, dry 10 mL Schlenk tube were added **4** (0.528 g, 2.394 mmol), potassium pentafluorobenzoate (0.8981 g, 3.590 mmol), CuI (0.0912 g, 0.479 mmol), and phenanthroline ligand (0.0863 g, 0.479 mmol). After three freeze–pump–thaw cycles, degassed diglyme (2.4 mL) was added via syringe, and the reaction was stirred for 10 min. The reaction was then heated to 130 °C for 40 h. After completion, the reaction was cooled to RT, diluted with DCM (to a volume of 10 mL), and passed through a silica plug. The product was purified by column chromatography (hexane/DCM), yielding orange crystalline solid **6** (318 mg, 43%). ^{1}H NMR (300 MHz, CD_2Cl_2): 6.79 (1 H, s), 4.27 (2 H, s), 4.14 (2 H, s). ^{19}F NMR (300 MHz, CD_2Cl_2): 140.70 (2 F, m), 156.57 (2 F, m), 162.88 (2 F, m). GC-MS (m/z): Found 308 (Calcd 307.98 for $[C_{12}H_5F_5S_2]$).

Compound M4. Compound **6** (290 mg, 308.29 mmol) was placed in a 20 mL vial with septa and purged with N_2. DCM (12 mL, 0.08 M) was added, and the reaction mixture was cooled to 0 °C. DDQ (426

dx.doi.org/10.1021/ma4019476 | *Macromolecules* 2013, 46, 8873–8881

Scheme 1. Synthesis of M1 and M2

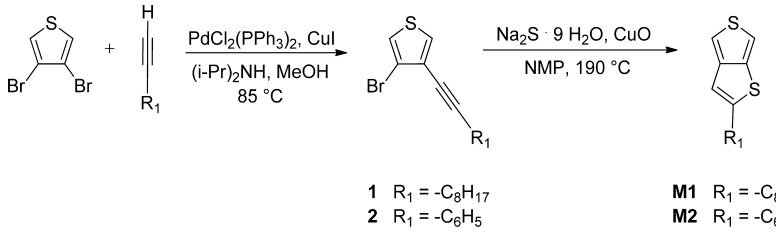

Scheme 2. Synthesis of M3 and M4

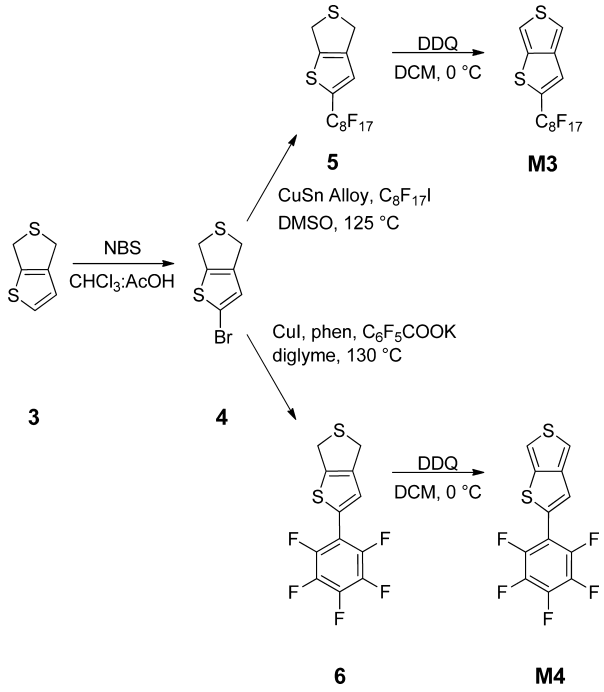

Scheme 3. Synthesis of M5

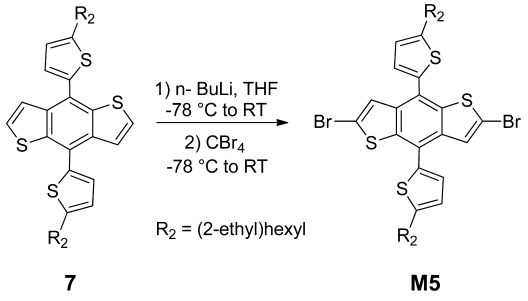

mg, 227.00 mmol) was added as a solid under a stream of N_2 and stirred for 30 min. Solvent was then removed, and the product was purified by column chromatography (hexanes, 0–7% DCM) yielding a white solid **M4** (152 mg, 53%). ^{1}H NMR (300 MHz, CD_2Cl_2): 7.57 (1 H, d, J = 4 Hz), 7.37 (1 H, d, J = 4 Hz), 7.35 (1 H, s). ^{19}F NMR (300 MHz, CD_2Cl_2): 139.35 (2 F, m), 154.63 (1 F, m), 162.50 (2 F, m). MS (EI+, m/z) Found 305.957, Calcd 305.9596 for $[C_{12}H_3F_5S_2]$.

Compound M5. Compound 7 (1.01 g, 1.84 mmol) and anhydrous THF (1.84 mL, 0.01 M) were added to a 500 mL flask equipped with addition funnel and cooled to −78 °C. *n*-BuLi in hexanes ([2.5] M, 1.84 mL, 4.60 mmol) was added dropwise, and the reaction was stirred for 1 h. The reaction went from yellow to light green to a blue-green fluorescent color. CBr_4 (1.52 g, 4.60 mmol) was added dropwise in dry THF (30 mL), and then the reaction became light brown as it was warmed to room temperature. Solvent was then removed under reduced pressure, and the product was diluted in ether, washed with H_2O, dried over anhydrous $MgSO_4$, and concentrated under vacuum. Purification by column chromatography (hexanes) and recrystallization from isopropanol yielded **M5** (1.09 g, 84%) as a yellow-orange solid. ^{1}H NMR (400 MHz, CD_2Cl_2): 7.66 (2 H, s), 7.21 (2 H, d), 6.92 (2 H, d), 2.90 (4 H, d), 1.78–1.73 (2 H, m), 1.54–1.42 (16 H, m), 1.07–1.00 (12 H, m). ^{13}C NMR (100 MHz, CD_2Cl_2): 146.44, 140.14, 135.95, 135.88, 128.00, 126.18, 125.65, 122.48, 116.76, 41.55, 33.86, 31.72, 28.97, 25.79, 23.15, 14.12, 10.81. MS (FAB+, m/z): Found 736.035, Calcd 736.080 for $[C_{18}H_6Br_2S_4]$.

Polymer Synthesis. PT8B. Into a Schlenk tube were added **M1** (0.252 g, 1 mmol), **M5** (0.7368 g, 1 mmol), $Pd_2(dba)_3{\cdot}CHCl_3$ (52 mg, 0.05 mmol), tris(2-methoxyphenyl)phosphine (70.5 mg, 0.2 mmol), pivalic acid (0.102 g, 1 mmol), and Cs_2CO_3 (0.9775 g, 3 mmol). The flask was then placed three times under vacuum and backfilled with N_2 gas after each evacuation. THF (10 mL, 0.1 M) was then added under a stream of N_2. The reaction mixture was stirred at room temperature for 30 min and then heated for 1 h. The flask was cooled to toom temperature, then $CHCl_3$ was added to fully dissolve the polymer, and the reaction solution was precipitated dropwise into cold, vigorously stirred methanol. The polymer was collected by filtration and subjected to sequential Sohxlet extraction with methanol, acetone, and hexanes. The polymer was then extracted with $CHCl_3$ and precipitated into methanol and isolated by filteration. The polymer solid was then dried under reduced pressure, yielding a shiny blue-black solid (716 mg, 86%). ^{1}H NMR (400 MHz, C_6D_5Cl, 110 °C): 7.88, 7.63, 7.47, 7.34, 2.88, 1.52, 1.32, 0.91. GPC: M_w 77.1 × 10^3 g/mol, $Đ$ 2.1.

PTPB, PTF8B, and PTFPB were synthesized according to the same procedure as described for PT8B. PTPB and PTFPB were also subjected to Sohxlet extraction with chlorobenzene to dissolve relatively higher molecular weight fractions. ^{1}H and ^{19}F NMR and gel permeation chromatography (GPC) data of the polymers are listed below. MALDI-TOF characterization of the polymer molecular weight and repeat unit weight is available in the Supporting Information.

PTPB. $CHCl_3$ soluble portion (171 mg, 22%). ^{1}H NMR (400 MHz, C_6D_5Cl, 110 °C): 7.94, 7.71, 7.56, 7.34, 3.07, 2.17, 1.46, 1.32, 0.91. GPC: M_w 18.7 × 10^3 g/mol, $Đ$ 1.5. C_6H_5Cl soluble portion (180 mg, 23%). GPC: M_w 32.0 × 10^3 g/mol, $Đ$ 1.5.

PTF8B. $CHCl_3$ soluble portion (155 mg, 68%). ^{1}H NMR (400 MHz, C_6D_5Cl, 110 °C): 7.90, 7.74, 7.55, 7.34, 3.10, 2.05, 1.54, 1.32, 0.91. ^{19}F NMR (300 MHz, $CDCl_3$, 22 °C): −80.83, −119.97, −121.88, −123.03, −126.34. GPC: M_w 22.6 × 10^3 g/mol, $Đ$ 1.3.

PTFPB. $CHCl_3$ soluble portion (91 mg, 52%). ^{1}H NMR (400 MHz, C_6D_5Cl, 110 °C): 7.95, 7.62, 7.52, 7.34, 3.01, 1.89, 1.43, 1.32, 0.91. ^{19}F NMR (300 MHz, $CDCl_3$, 22 °C): −153.26 to −185.37 (b). GPC: M_w 22.7 × 10^3 g/mol, $Đ$ 1.9. C_6H_5Cl soluble portion (43 mg, 25%). GPC: M_w 36.8 × 10^3 g/mol, $Đ$ 1.9.

3. RESULTS AND DISCUSSION

3.1. Synthesis. The corresponding thieno[3,4-*b*]thiophene and dibromobenzodithiophene monomers **M1**–**M5** were synthesized as shown in Schemes 1–3. Direct arylation polymerization, as shown in Scheme 4, was selected in order to eliminate extra synthetic steps to synthesize the dibrominated thienothiophene and distannylated benzodithiophene units. Brominated thienothiophenes units are generally unstable

dx.doi.org/10.1021/ma4019476 | Macromolecules 2013, 46, 8873–8881

Scheme 4. Synthesis of PT8B, PTPB, PTF8B, and PTFPB

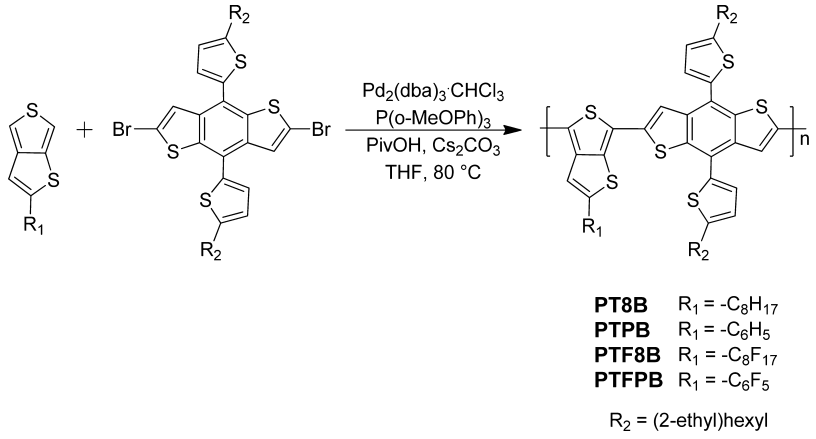

in air and difficult to store for long periods of time. Additionally, production of distannylated monomers involves the use of highly toxic reagents resulting in products that are difficult to purify and handle. Eliminating extra steps simplifies the synthesis and increases the overall process yield.

The nonfluorinated units, **M1** and **M2**, were synthesized via a relatively simple, scalable, two-step method which has been previously described (Scheme 1).[21,22] First, 3,4-dibromothiophene was selectively coupled with the corresponding terminal alkyne via Sonagashira coupling, yielding compounds **1** and **2** in 44% and 43% yields, respectively. Subsequently, cyclization of **1** and **2** was performed with sodium sulfide at elevated temperatures in the presence of CuO, yielding **M1** and **M2** in 44% and 22% yields, respectively. This route affords alkyl-substituted thienothiophene monomers via a direct and simplified synthesis, in contrast to the longer and more difficult synthetic routes for thienothiophene monomers which contain ketone or ester substituents and require several more synthetic steps.[23]

Synthesis of the perfluorinated side chain thienothiophene analogues, **M3** and **M4**, was accomplished through the use of the dihydrothieno[3,4-*b*]thiophene (**3**) synthetic building block as shown in Scheme 2. Synthesis of **3** has been reported previously in the literature;[18] however, this is the first example of its use as a building block to achieve differently substituted thienothiophene monomers. Bromination of **3** in a 1:1 mixture of $CHCl_3$ and acetic acid quantitatively yielded **4**, which could then be used with existing coupling methods developed for thiophene derivatives to give **5** and **6**.[19,24] Oxidation of **5** and **6** with DDQ then yielded the desired fluorinated monomers **M3** and **M4**, respectively. We note that **3** or **4** could be used with a wide variety of existing coupling chemistries to synthesize many other new thienothiophene derivatives.

The dithienylbenzodithiophene block (**7**) was synthesized as reported.[20] Selective bromination was achieved by lithiation of the two α-thiophene positions on **7**, followed by the addition of CBr_4 to give the brominated product **M5** in good yield, 84%. This bromination methodology has been previously reported for similar benzodithiophene derivatives.[25]

Next, utilizing the activated C−H bonds of the thienothiophene monomers (**M1**−**M4**) and the aryl halide bonds in the dibrominated benzodithiophene monomer (**M5**), a series of alternating copolymers were synthesized (Scheme 4) via optimized direct arylation polymerization conditions (see Supporting Information). Polymerization proceeded rapidly using the $Pd_2(dba)_3{\cdot}CHCl_3$ and tris(2-methoxyphenyl)-phosphine catalyst system in THF.[17i] After 1 h of reaction time at moderate temperatures, polymers were achieved with 18−77 kDa weight-average molecular weights by GPC versus polystyrene standards. Prolonged reaction times were found to increase the portion of insoluble material, presumably because of cross-linking at either the 3-thieno[3,4-*b*]thiophene position or β-thiophene positions on benzodithiophene. The polymers were purified via sequential Soxhlet extraction, yielding materials that all were equally soluble in chloroform. Higher molecular weight fractions of PTPB and PTFPB were dissolvable in chlorobenzene. Interestingly, as a result of the perfluorinated side chains, PTF8B was more soluble in THF and less soluble in chlorinated aromatic solvents compared to the rest of the PTB series.

Table 1. Polymer Molecular Weight Analysis by GPC

polymer	M_n[b] (kDa)	M_w[b] (kDa)	$Đ$	yield (%)
PT8B	37.4	77.1	2.1	86[d]
PTPB	12.8	18.7	1.5	22[d]
PTPB	21.4	32.0	1.5	23[e]
PTF8B	17.9[c]	22.6[c]	1.3	68[d]
PTFPB	12.0	22.7	1.9	52[d]
PTFPB	18.9	36.8	1.9	25[e]

[a]Reactions were performed at 80 °C for 1 h in THF (0.1 M), $Pd_2(dba)_3$ $CHCl_3$ (5 mol %), P(*o*-MeOPh)$_3$ (20 mol %), pivalic acid (1 equiv), and Cs_2CO_3 (3 equiv). [b]Calculated by GPC in 1,2,4-trichlorobenzene at 135 °C using PS standards. [c]Calculated by GPC in THF using PS standards. [d]Calculated from $CHCl_3$ soluble portion. [e]Calculated from chlorobenzene soluble portion.

The structures of the polymers were analyzed and confirmed using NMR and MALDI-TOF mass spectroscopy. Elevated temperatures were required to collect ^{1}H NMR spectra due to aggregation of the polymers in solution. MALDI-TOF spectra showed good alternating structure in each of the polymers, and the calculated masses for the repeat units of the polymers corresponded closely to the observed peaks (see Supporting Information), positively confirming the polymer structures. However, absolute molecular weight and distribution measurements were not calculated from these measurements, since higher molecular weight conjugated polymers are typically difficult to detect in MALDI-TOF due to fragmentation.

3.2. Molecular Orbital and Ground-to-Excited State Dipole Change ($\Delta\mu_{ge}$) Calculations. Computations were

dx.doi.org/10.1021/ma4019476 | *Macromolecules* 2013, 46, 8873−8881

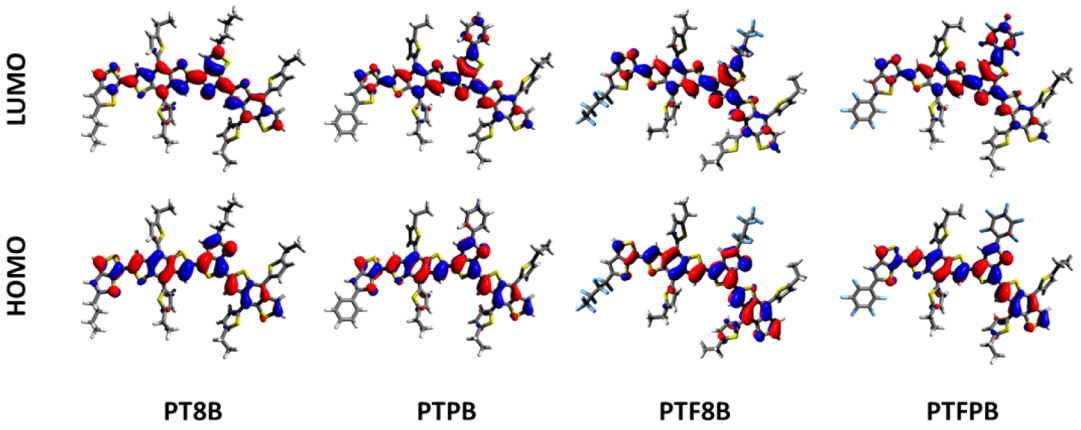

Figure 3. Molecular orbitals for D−A polymer dimer models (n = 2).

performed in order to model the effect of the perfluorinated groups on the HOMO/LUMO molecular orbitals (Figure 3), to predict the E_{HOMO}/E_{LUMO} levels, and to estimate the $\Delta\mu_{ge}$ (Table 2). Excited- and ground-state DFT computations, with the polymers modeled as dimers (n = 2), were performed at the hybrid density functional level B3LYP/6-31G(d,p) in Gaussian09.[26]

Table 2. Computational Modeling of E_{HOMO}, E_{LUMO}, and $\Delta\mu_{ge}$

polymer	E_{HOMO}[a] (eV)	E_{LUMO}[a] (eV)	E_g[a] (eV)	$\Delta\mu_{ge}$[b] (D)
PT8B	−4.60	−2.10	2.50	2.34
PTPB	−4.66	−2.21	2.45	8.24
PTF8B	−4.95	−2.48	2.46	11.18
PTFPB	−4.81	−2.43	2.38	18.15

[a]Computed with B3LYP/6-31G(d,p) using dimer structure (n = 2). [b]Computed with B3LYP/6-31G(d,p) using monomer structure (n = 1).

As seen in the molecular orbital diagrams of Figure 3, the HOMOs are delocalized over the entire backbone in each case, while the LUMOs have more electron density localized upon the thienothiophene unit, particularly in the cases with the perfluorinated groups, PTF8B and PTFPB. Additionally, for PTPB and PTFPB, the phenyl group is nearly planar with the thienothiophene unit, giving further delocalization of electron density and leading to relatively lower bandgaps. The effect of this extended conjugation is observable in the LUMO density maps by the nonzero contributions of the pendant phenyl groups. This is also reflected in the computed energy levels, where the effect of the extended conjugation into the aryl group is small, but observable, leading to slightly reduced bandgaps by 0.05−0.12 eV. Computational evaluation of the polymers shows a significant electron withdrawing effect upon incorporation of perfluorinated groups, which is shown by a lowering in both the E_{HOMO} and E_{LUMO}.

Previously, Yu et al. noted a positive correlation between increased PCE and larger computed values $\Delta\mu_{ge}$, which were calculated by the semiempirical AM1 method.[12a,b] Semiempirical methods for conjugated D−A molecules have been shown to underestimate $\Delta\mu_{ge}$.[28] Our own independent calculations confirm this underestimation for AM1 when evaluating a portion of the same reported set of diphenylacetylene donor−acceptor small molecules (Figure S33).[28] Additionally, calculations using B3LYP/6-31G(d,p) for the same molecules were shown to overestimate $\Delta\mu_{ge}$ compared to experimental results (Table S3a). The ground state dipole moments and excited state dipole moments were taken from ground state SCF density and the excited state TDDFT CI density, respectively. The ground-to-excited state dipole changes were calculated from the previously reported relationship $\Delta\mu_{ge} = [(\mu_{ge} - \mu_{ex})^2 + (\mu_{gy} - \mu_{ey})^2 + (\mu_{gz} - \mu_{ez})^2]$.[12] The two methods agree fairly well when calculating the ground state dipole moment, so the difference is attributed to excited state dipole moment calculations. This comparative evaluation can be found in the Supporting Information (Table S3b).

In order to understand how $\Delta\mu_{ge}$ changes with structural variations in this study, the ground and excited state dipole moments were calculated using B3LYP/6-31G(d,p). $\Delta\mu_{ge}$ was calculated for the polymers (with n = 1) using the method described above (Table 2). The fluorinated pendants were found to greatly increase $\Delta\mu_{ge}$ by approximately 10 D compared to the nonfluorinated analogues. The $\Delta\mu_{ge}$ was also increased by 5−6 D by extending the conjugation away from the polymer backbone with the incorporation of phenyl pendants in the cases of PTPB and PTFPB. The $\Delta\mu_{ge}$ was the highest, 18.15 D, for PTFPB where the fluorine atoms were directly bonded to the conjugated system. For comparison, $\Delta\mu_{ge}$ was calculated for a series of reported polymers prepared by Yu et al. (Figure 4) using the B3LYP/6-31G(d,p) method.[12a,15] The calculated $\Delta\mu_{ge}$ values for the reported materials PBB3, PTBF2, PTB2 and PTB7 were 4.12, 13.5, 15.7, and 14.84 D, respectively (Table S4). The new PTB series have

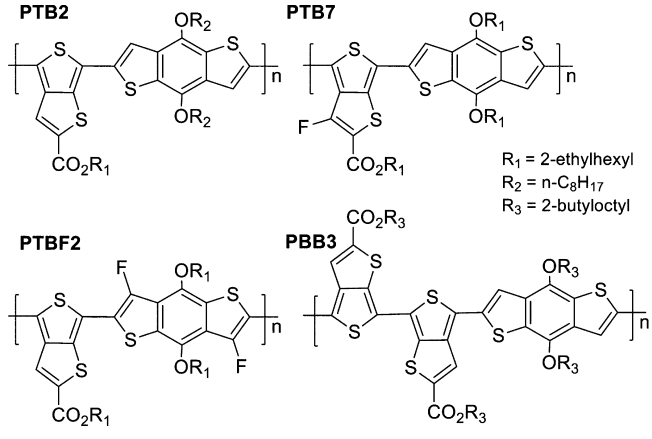

Figure 4. Structures of reported polymers used for comparison.[12a,15]

dx.doi.org/10.1021/ma4019476 | Macromolecules 2013, 46, 8873−8881

$\Delta\mu_{ge}$ values that span an even wider range overall, from 2.34 to 18.15 D. The PTB series will provide an opportunity to evaluate the observed correlation of $\Delta\mu_{ge}$ and PCE in a new set of materials and determine if $\Delta\mu_{ge}$ is a critical factor for improving device efficiencies. If this trend applies to these materials, $\Delta\mu_{ge}$ could potentially be used in future research as an easily computable value for designing and screening new conjugated materials.

It is interesting to speculate about the nature of $\Delta\mu_{ge}$ and the structural features of a polymer that may increase or decrease the ground and excited state dipoles and also how $\Delta\mu_{ge}$ will be changed when considering greater chain lengths resembling polymers. Most computations of $\Delta\mu_{ge}$ have been performed using a monomeric model system where n = 1. In one single repeat unit the possibility of dipole cancellation created by other acceptor units is avoided. At chain lengths greater than n = 1 this effect could be significant, especially since these polymers have off-axis pendant functionality which could cancel the overall outward moment contributions. To investigate this, computations were performed with n = 2 and n = 2.5. The n = 2.5 systems in contrast to the n = 2 and n = 1 systems are symmetrical with each electron acceptor in the same chemical environment (D−A−D−A−D). In both cases with n = 2 and n = 2.5 the magnitude of $\Delta\mu_{ge}$ decreases significantly as expected, yet the main trends are preserved by comparison to the n = 1 models (Table S5). Investigating $\Delta\mu_{ge}$ as a function of n could provide more of an understanding of the effects of $\Delta\mu_{ge}$ on polymeric systems when compared with experimental data or could suggest using $\Delta\mu_{ge}$ with caution if there are qualitative differences between trends using different n.

3.3. Optical and Electrochemical Properties of the Polymers. The optical absorption and electrochemical analyses demonstrate significant changes in the electron density as a result of changing from octyl to phenyl and from adding the fluorinated pendent groups along the backbone. The electron withdrawing nature of the different thienothiophene units were examined using cyclic voltammetry (CV) as shown in Figure 5. The measured E_{HOMO} levels for PT8B, PTPB, PTF8B, and PTFPB are −5.13, −5.10, −5.35, and −5.24 eV, respectively. These results were supported by both density functional theory calculations (Table 2) and ultraviolet photoelectron spectroscopy (UPS) measurements (Table 3). Both experimental and computational results show that the perfluorinated units TF8 and TFP have lower E_{HOMO} levels due to the strong electron withdrawing nature of the fluorine atoms. The thienothiophene units display the following trend for the least to most electron withdrawing T8 ≈ TP < TFP < TF8. The reduction of the E_{HOMO} level following fluorine substitution has been well documented, and these results correspond well to previous literature reports.[11,12] Directly comparing the polymers with nonfluorinated and perfluorinated side groups, the TF8 unit reduces the E_{HOMO} by 0.22 eV versus the T8 unit, while the TFP unit reduces the E_{HOMO} by 0.14 eV relative to the TP unit.

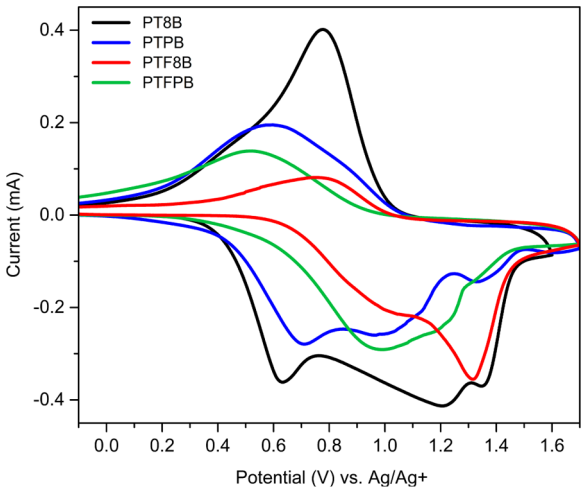

Figure 5. Cyclic voltammograms of the oxidation onsets of PT8B, PTPB, PTF8B, and PTFPB films. Films were drop-cast from chloroform (2.5 mg/mL) solutions onto the working electrode.

Figure 6 shows the ultraviolet−visible (UV−vis) absorption spectroscopy of each of the polymers in dilute solution ($CHCl_3$) and as thin films. Each of the polymers absorb strongly in the region from ∼500 to 750 nm. Using the onset of absorption in the thin films, the optical bandgaps for PT8B, PTPB, PTF8B, and PTFPB were calculated (Table 3). The extended conjugation in the TP and TFP units broaden the polymer absorption, lowering the band gap by 0.07−0.11 eV. The lowest band gap is observed in PTFPB, potentially due to the increased aggregation and interchain interactions created by the addition of the perfluorinated phenyl group. The extinction coefficients for PT8B and PTPB were quite high (10^5 cm^{-1}) while those for PTF8B and PTFPB were slightly lower.

It is apparent that there is a much larger shift, from solution to film, in the λ_{max} and λ_{onset} for both PT8B and PTPB compared to the perfluorinated polymers PTF8B and PTFPB. Commonly this shift in due to increased aggregation in the solid state. It is interesting that the polymers with perfluorinated side chains do not exhibit much of a shift when comparing the solution and film absorption. This is likely the result of the stronger interchain interactions and aggregation in solution which are induced by the presence of the perfluorinated groups. Generally, increased interchain interactions create smaller π−π stacking distances, greater charge mobilities, and higher crystallinity in the solid state.

From the absorption onsets of the polymer films and the oxidation potential onsets, the E_{LUMO} was calculated and the bandgaps were determined for each of the polymers (Figure 7). Each of the polymers displays a low-lying E_{HOMO} which can be attributed mainly to the dithienyl-substituted benzodithiophene donor unit. Addition of the flanking thiophene units has been shown to lower the E_{HOMO}, creating polymers with higher V_{oc} and greater oxidative stability.[20] Changing from alkyl to aryl substituents on the thienothiophene unit slightly lowers the bandgap (by 0.08 to 0.11 eV) which can be attributed to either the extended conjugation or the different electron withdrawing nature of the pendent groups. Replacement of the alkyl pendent groups with perfluorinated pendent groups induces a significant lowering of both the E_{HOMO} (0.14−0.22 eV) and E_{LUMO} (0.22−0.26 eV). Additionally, in comparison, the experimental orbital energies agree very well with computational data after applying an empirical correction factor of −0.45 ± 0.06 eV for the E_{HOMO} levels and −1.26 ± 0.05 eV for the E_{LUMO} levels (uncertainties are standard deviations in the tested data set).

The "ideal" low bandgap polymer energy levels in Figure 7 are based on the following requirements: (1) high $E_{HOMO}^{polymer}/E_{LUMO}^{PCBM}$ level offset to promote high V_{oc}, (2) low bandgap for good absorption of the solar spectrum for a high J_{sc}, and (3) appropriate $E_{LUMO}^{polymer}/E_{LUMO}^{PCBM}$ level offset (>0.3 eV) for donor−

dx.doi.org/10.1021/ma4019476 | Macromolecules 2013, 46, 8873−8881

Table 3. Optical and Electrochemical Properties of Donor−Acceptor Copolymers

	UV−vis absorption							E_{HOMO} measurement	
	solution			film					
polymer	λ^{max} (nm)	λ^{onset} (nm)	E_g^{opt} (eV)	λ^{max} (nm)	λ^{onset} (nm)	E_g^{opt} (eV)	abs coeff[c] (cm^{-1})	E_{HOMO}^{CV} [a] (eV)	E_{IP}^{UPS} [b] (eV)
PT8B	600, 650	700	1.77	607, 665	725	1.71	1.09×10^5	−5.13	−4.75
PTPB	620, 675	733	1.69	633, 687	760	1.63	1.01×10^5	−5.10	−4.76
PTF8B	615, 667	733	1.69	620, 669	740	1.68	8.0×10^4	−5.35	−5.09
PTFPB	630, 693	783	1.58	624, 694	795	1.56	7.4×10^4	−5.24	−4.99

[a]Versus Fc/Fc^+ external reference. [b]Measured on ITO-coated substrate. [c]Calculated using polymer film.

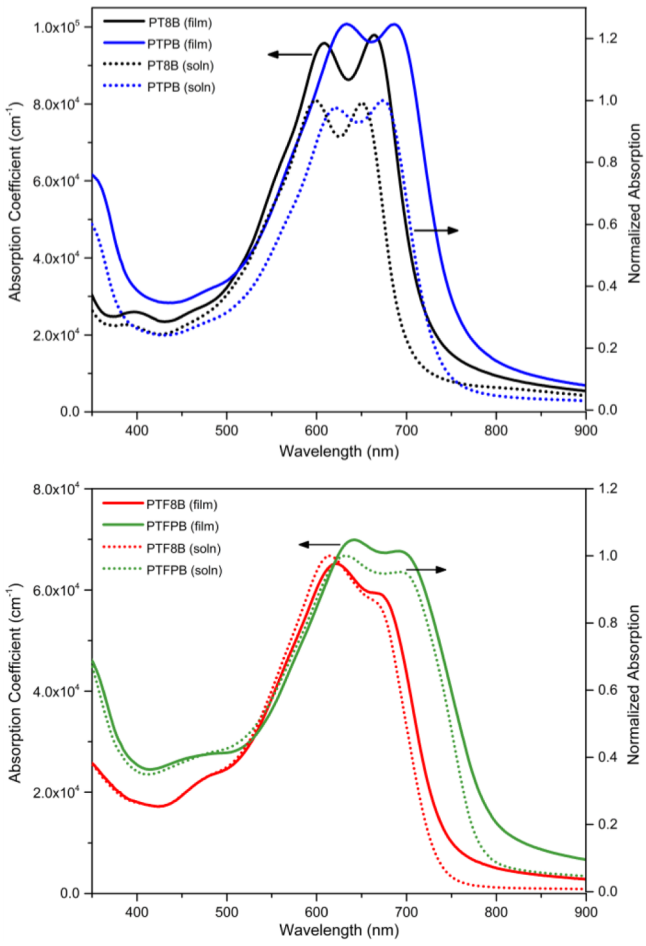

Figure 6. (top) Absorption spectra of PT8B, PTPB, (bottom) PTF8B, and PTFPB. Solutions were in chloroform (~0.01 mg/mL). Films were spin-coated from chloroform solutions (10 mg/mL). Absorption coefficients were calculated using polymer films; film thicknesses were determined with a surface profilometer.

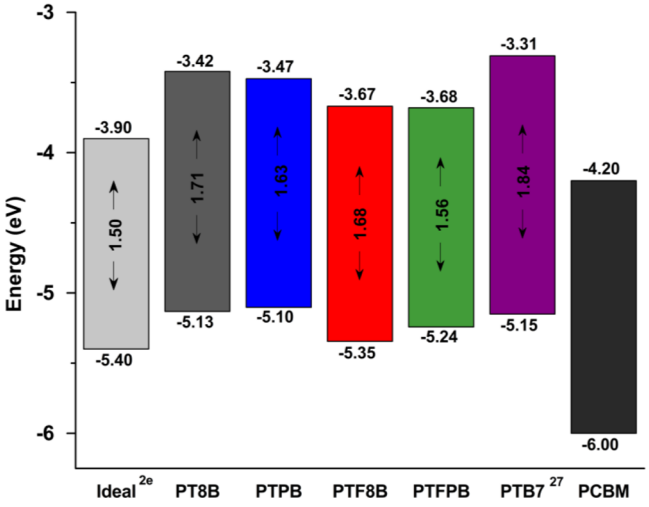

Figure 7. Cyclic voltammetry derived E_{HOMO} and E_{LUMO} levels and optical E_g for PT8B, PTPB, PTF8B, and PTFPB. Energy levels of an "ideal" low bandgap polymer and $PC_{61}BM$ are listed for comparison.[2e]

acceptor charge transfer. The synthesized PTB polymers compare well to these ideal energy levels and have potential to function well in an OPV device. Relative to a recent high performing low bandgap polymer, PTB7,[27] it can be seen that the PTB polymer series displays similar or slightly lower E_{HOMO} levels and lower bandgaps.

PTF8B and PTFPB should display significantly different morphologies when mixed with PCBM compared to PT8B and PTPB. Studies of the polymer/PCBM blends and their morphology, crystallinity, domain size/purity and PCBM miscibility are ongoing. The PTB series should offer interesting insight into the effect of fluorine on conjugated low bandgap polymers and provide information for the future design of polymers for OPVs.

4. CONCLUSION

We report the design, synthesis, and characterization of a new series of thienothiophenebenzodithiophene alternating copolymers with octyl (PT8B), phenyl (PTPB), perfluorooctyl (PTF8B), or perfluorophenyl (PTFPB) side groups on the thienothiophene unit. The phenyl units were found to increase the conjugation area, leading to relatively lower bandgaps. The perfluorinated groups increased the electron withdrawing nature of the thienothiophene acceptor unit, decreasing the E_{HOMO} and E_{LUMO} levels and enhancing the calculated $\Delta\mu_{ge}$. The PTB series have good absorption over the visible/near-IR spectrum, strong absorption coefficients, and appropriately aligned energy levels compared to "ideal" polymer energy levels, which should translate to strongly performing electronic materials. Further studies to investigate the effect of perfluorinated groups on the morphology, mobility, and device performance are currently in progress and will be reported upon completion.

■ ASSOCIATED CONTENT

Supporting Information

NMR, MALDI-TOF, and UPS spectra along with computational results. This material is available free of charge via the Internet at http://pubs.acs.org.

dx.doi.org/10.1021/ma4019476 | Macromolecules 2013, 46, 8873−8881

AUTHOR INFORMATION

Corresponding Author

*E-mail Coughlin@mail.pse.umass.edu (E.B.C.).

Notes

The authors declare no competing financial interest.

ACKNOWLEDGMENTS

This work is supported as part of Polymer-Based Materials for Harvesting Solar Energy (PHaSE), an Energy Frontier Research Center funded by the U.S. Department of Energy, Office of Science, Office of Basic Energy Sciences, under Award DE-SC0001087. Mass spectral data for all materials were obtained at the University of Massachusetts Mass Spectrometry Center.

REFERENCES

(1) Yu, G.; Gao, J.; Hummelen, J. C.; Wudl, F.; Heeger, A. J. *Science* **1995**, *270*, 1789.

(2) (a) Krebs, F. C.; Gevorgyan, S. A.; Alstrup, J. *J. Mater. Chem.* **2009**, *19*, 5442. (b) Cheng, Y. J.; Yang, S. H.; Hsu, C.-S. *Chem. Rev.* **2009**, *109*, 5868. (c) Liang, Y.; Yu, L. *Acc. Chem. Res.* **2010**, *43*, 1227. (d) Son, H. J.; Carsten, B.; Jung, I. H.; Yu, L. *Energy Environ. Sci.* **2012**, *5*, 8158. (e) Zhou, H.; Yang, L.; You, W. *Macromolecules* **2012**, *45*, 607. (f) Mei, J.; Diao, Y.; Appleton, A. L.; Fang, L.; Bao, Z. *J. Am. Chem. Soc.* **2013**, *135*, 6724. (g) Zhu, X. H.; Peng, J.; Cao, Y.; Roncali, J. *Chem. Soc. Rev.* **2011**, *40*, 3509.

(3) Liang, Y.; Danqin, F.; Wu, Y.; Tsai, S. T.; Li, G.; Ray, C.; Yu, L. *J. Am. Chem. Soc.* **2009**, *131*, 7792.

(4) Chen, H. Y.; Hou, J.; Zhang, S.; Liang, Y.; Yang, G.; Yang, Y.; Yu, L.; Wu, Y.; Li, G. *Nat. Photonics* **2009**, *3*, 649.

(5) Yang, Y.; et al. *Nat. Photonics* **2012**, *6*, 180.

(6) He, Z.; Zhong, C.; Su, S.; Zu, M.; Wu, H.; Cao, Y. *Nat. Photonics* **2012**, *6*, 591.

(7) Yang, Y.; et al. *Nat. Commun.* **2013**, *4*, 1446.

(8) Li, W.; Furlan, A.; Hendriks, K. H.; Wienk, M. M.; Janssen, R. A. *J. Am. Chem. Soc.* **2013**, *135*, 5529.

(9) He, Z.; Zhong, C.; Huang, X.; Wong, W.; Wu, H.; Chen, L.; Su, S.; Cao, Y. *Adv. Mater.* **2011**, *23*, 4636.

(10) Ye, L.; Zhang, S.; Ma, W.; Fan, B.; Guo, X.; Huang, Y.; Ade, H.; Hou, J. *Adv. Mater.* **2012**, *23*, 6335.

(11) (a) Zhou, H.; Yang, L.; Stuart, A. C.; Price, S. C.; Liu, S.; You, W. *Angew. Chem.* **2011**, *50*, 2995. (b) Price, S.; Stuart, A. C.; Yang, L.; Zhou, H.; You, W. *J. Am. Chem. Soc.* **2011**, *133*, 4625. (c) Li, Z.; Jianping, L.; Tse, S. C.; Zhou, J.; Xiaomei, Du.; Tao, Y.; Ding, J. *J. Mater. Chem.* **2011**, *21*, 3226. (d) Chen, H. C.; Chen, Y. H.; Liu, C. C.; Chien, Y. C.; Chou, S. W.; Chou, P. T. *Chem. Mater.* **2012**, *24*, 4766. (e) Wu, F.; Zha, D.; Chen, L.; Chen, Y. *Polym. Chem.* **2013**, *51*, 1506. (f) Schroeder, B.; Huang, Z.; Ashraf, R. S.; Smith, J.; D'Angelo, P.; Watkins, S. E.; Anthopoulos, T. D.; Durrant, J. R.; McCulloch. *Adv. Funct. Mater.* **2012**, *22*, 1663. (g) Bronstein, H.; Frost, J. M.; Hadipour, A.; Kim, Y.; Nielsen, C. B.; Ashraf, R. S.; Rand, B. P.; Watkins, S.; McCulloch, I. *Chem. Mater.* **2013**, *25*, 277.

(12) (a) Carsten, B.; Szarko, J. M.; Son, H. J.; Wang, W.; Lu, L.; He, F.; Rolczynski, B. S.; Lou, S. J.; Chen, L. X.; Yu, L. *J. Am. Chem. Soc.* **2011**, *133*, 20468. (b) Carsten, B.; Szarko, J. M.; Lu, L.; Son, H. J.; Botros, Y. Y.; Chen, L. X.; Yu, L. *Macromolecules* **2012**, *45*, 6390. (c) Stuart, A. C.; Tumbleston, J. R.; Zhou, H.; Li, W.; Liu, S.; Ade, H.; You, W. *J. Am. Chem. Soc.* **2013**, *135*, 1806.

(13) Okamoto, T.; Nakahara, K.; Saeki, A.; Seki, S.; Oh, J. H.; Akkerman, H. B.; Bao, Z.; Matsuo, Y. *Chem. Mater.* **2011**, *23*, 1646.

(14) Yang, L.; Tumbleston, J. R.; Zhou, H.; Ade, H.; You, W. *Energy Environ. Sci.* **2013**, *6*, 316.

(15) Tumbleston, J. R.; Stuart, A. C.; Gann, E.; You, W.; Ade, H. *Adv. Funct. Mater.* **2013**, DOI: 10.1002/adfm.201300093.

(16) (a) Mercier, L. G.; Leclerc, M. *Acc. Chem. Res.* **2013**, DOI: 10.1021/ar3003305. (b) Schipper, D. J.; Fagnou, K. *Chem. Mater.* **2011**, *23*, 1594. (c) Facchetti, A.; Vaccaro, L.; Marrocchi, A. *Angew. Chem., Int. Ed.* **2012**, *51*, 3520.

(17) (a) Wang, Q.; Takita, R.; Kikuzaki, Y.; Ozawa, F. *J. Am. Chem. Soc.* **2010**, *132*, 11420. (b) Lu, W.; Kuwabara, J.; Kanbara, T. *Macromolecules* **2010**, *44*, 1252. (c) Kowalski, S.; Allard, S.; Scherf, U. *ACS Macro Lett.* **2012**, *1*, 465. (d) Allard, N.; Najari, A.; Pouliot, J.; Pron, A.; Grenier, F.; Leclerc, M. *Polym. Chem.* **2012**, *3*, 2875. (e) Chang, S. W.; Waters, H.; Kettle, J.; Kuo, Z. R.; Li, C. H.; Yu, C. Y.; Horie, M. *Macromol. Rapid Commun.* **2012**, *33*, 1927. (f) Wang, Q.; Wakioka, M.; Ozawa, F. *Macromol. Rapid Commun.* **2012**, *14*, 1203. (g) Fujinami, Y.; Kuwabara, J.; Lu, W.; Hayashi, H.; Kanbara, T. *ACS Macro Lett.* **2012**, *1*, 67. (h) Wang, D. H.; Pron, A.; Leclerc, M.; Heeger, A. J. *Adv. Funct. Mater.* **2013**, *23*, 1297. (i) Wakioka, M.; Kitano, Y.; Ozawa, F. *Macromolecules* **2013**, *46*, 370.

(18) Dey, T.; Navaranthne, D.; Invernale, M. A.; Berghorn, I. A.; Sotzing, G. A. *Tetrahedron Lett.* **2010**, *51*, 2069.

(19) Shang, R.; Fu, Y.; Wang, Y.; Xu, Q.; Yu, H. Z.; Liu, L. *Angew. Chem., Int. Ed.* **2009**, *48*, 9350.

(20) Huo, L.; Zhang, S.; Guo, X.; Xu, F.; Li, Y.; Hou, J. *Angew. Chem., Int. Ed.* **2011**, *50*, 9697.

(21) Bae, W. J.; Scilla, C.; Duzhko, V. V.; Jo, W. H.; Coughlin, E. B. *J. Polym. Sci., Part A* **2011**, *49*, 3260.

(22) Lee, W. S.; Park, J. H.; Lee, Y. S.; Lee, S. H.; Pyo, M.; Zong, K. *Synth. Met.* **2010**, *160*, 1368.

(23) Hou, J.; Chen, H. Y.; Zhang, S.; Chen, R. I.; Yang, Y.; Wu, Y.; Li, G. *J. Am. Chem. Soc.* **2009**, *131*, 15586.

(24) Facchetti, A.; Yoon, M. H.; Stern, C. L.; Hutchison, G. R.; Ratner, M. A.; Marks, T. J. *J. Am. Chem. Soc.* **2004**, *126*, 13480.

(25) Hundt, N.; Palaniappan, J.; Servello, J.; Dei, D. K.; Stefan, M. C.; Biewer, M. C. *Org. Lett.* **2009**, *11*, 4422.

(26) Frisch, M. J.; et al. *Gaussian 09, Revision B.01*; Gaussian Inc.: Wallingford, CT, 2009.

(27) Liang, Y.; Xu, Z.; Xia, J.; Tsai, S. T.; Wu, Y.; Li, G.; Ray, C.; Yu, L. *Adv. Mater.* **2010**, *22*, E135.

(28) Dehu, C.; Meyers, F.; Bredas, J. L. *J. Am. Chem. Soc.* **1993**, *115* (14), 6198–6206.

(29) Stiegman, A. E.; Graham, E.; Perry, K. J.; Khundkar, L. R.; Cheng, L. T.; Perry, J. W. *J. Am. Chem. Soc.* **1991**, *113* (20), 7658–7666.